Research Article

Eivind Hugaas* and Andreas T. Echtermeyer

Filament wound composite fatigue mechanisms investigated with full field DIC strain monitoring

https://doi.org/10.1515/eng-2021-0041
Received Jul 21, 2020; accepted Nov 25, 2020

Abstract: Fatigue of filament wound materials was investigated using Digital Image Correlation DIC monitoring every 50^{th} cycle of a high cycle fatigue test of a split disk ring sample. The ring was cut from a filament wound glass fiber reinforced polymer pressure vessel and had a hole. The strain field redistributed over time, lowering and moving strain concentrations. The redistributive behavior was most extensive in areas that later developed local fiber failure, which soon led to catastrophic failure. Microscopy was carried out on partially fatigued material. Damage evolved as matrix cracks and matrix splitting of groups of fibers and complete debonding of single fibers. This occurred at borders of voids and matrix cracks, easing progressive fiber failure. It was concluded that fatigue in filament wound composites has an extensive matrix damage phase before final failure. Fibers could locally withstand strains close to and above the static failure strain for considerable number of cycles if little local strain field redistribution was observed. The used method was able to detect changes in the strain fields that preceded catastrophic failure. It was concluded that DIC combined with the post processing methods presented may serve as a valuable tool for structural integrity monitoring of composite pressure vessels over time.

Keywords: Composites; Filament Winding; Fatigue; Digital Image Correlation; Progressive damage; Strain Fields

1 Introduction

Composite pressure vessels are widely used for transporting and storing gas, especially hydrogen. Understanding how fatigue damage initiates and grows is critical for this application and for further development of predictive models. The current design/verification standards demand full scale testing of every new pressure vessel design driving up development cost. Additionally there are very tight tolerances on wear and damage from use, leading to potential premature decommissioning. A better understanding of the long-term properties can optimize the use of composite materials and simplify the testing requirements, giving leaner and cheaper designs [1–6].

Testing of composite pressure vessels can be simplified by testing of curved filament wound samples as an alternative to tedious full scale testing of the vessels. Currently, the split disk method is perhaps the most pragmatic and easy to use. The method does introduce complexities that need addressing. Most critical being the influence of the split on the through thickness strain fields. Prior research suggests that the strain concentration introduced through friction between the split of the disk and the specimen is negligible provided that the friction between sample and disk is low [7, 8]. However, through thickness strain concentrations will arise from bending [9]. These will be located at the outside surface at the split and inside surface at the center, as indicated in green squares and lines in Figure 1. The hole in the specimen was introduced to further concentrate the strain simulating damage in a pressure vessel. The hole concentrates the strain to four known points as indicated by black circles in Figure 1.

The non-homogenous nature of composites, such as variations in the fiber and matrix distribution, makes traditional single point strain monitoring methods insufficient, such as strain gauges. Knowledge of the entire strain field would be needed. This particularly applies when studying damage evolution, where strain fields may change over time due to progressive damage development. With the advent of ever larger processing power of computers it is now possible to use full field strain monitoring technologies with a data acquisition frequency suitable for fatigue testing. One such high-resolution monitoring method is Digital Image Correlation (DIC) strain monitoring.

Matrix voids and layer thickness in particular tend to vary extensively throughout the layup when using filament winding [10]. Layer thickness will naturally affect the local

***Corresponding Author: Eivind Hugaas:** Norwegian University of Science and Technology, NTNU Trondheim, Norway; Email: eivindh_5@hotmail.com
Andreas T. Echtermeyer: Norwegian University of Science and Technology, NTNU Trondheim, Norway

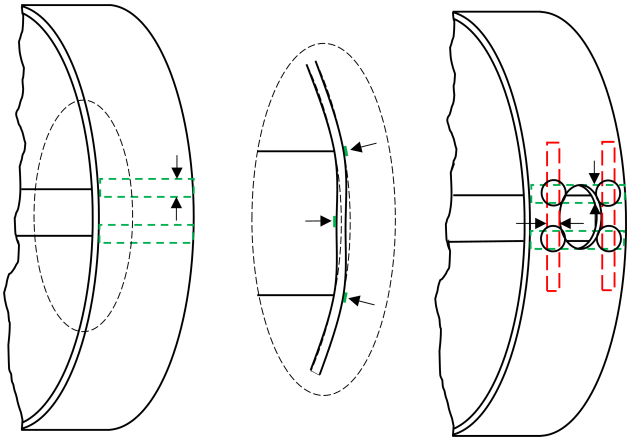

Figure 1: Schematic illustrating the strain concentration from bending in a split disk sample in green squares and lines and the further concentration introduced with a hole. Arrows and circles further highlight the strain concentrations.

strain fields through varying amounts of loadbearing material. Matrix voids affect the mechanical properties and strength of unidirectional composite materials to a great extent, particularly under cyclic loading, as shown by several recent publications [11–15]. It is therefore to be expected that fatigue damage in a filament wound component will be dominated by matrix damage and also have a considerable scatter and variation in mechanical properties, lifetime and strain fields. The possible spatial variation of properties makes DIC a particularly useful monitoring method, since DIC can monitor the entire surface of the test specimen.

DIC has been shown to be a powerful tool for monitoring composite fatigue. Prior studies utilizing DIC [16–18] have concluded that there is extensive strain field evolution and damage development throughout the fatigue life. Post processing high frequency DIC data is however computationally expensive. Little effort has so far been made to tailor the post processing to better highlight fatigue damage growth of composites besides acknowledging that it can be extensive and progressive. For static properties however, some efforts have been made. He *et al.* [19] used DIC of short beam shear tests combined with a finite element iterative algorithm to find mechanical constants. He's algorithm matched the FEA strain field with the DIC strain field by iteratively changing the mechanical constants and a consistent convergence was found.

DIC is a good candidate for structural integrity monitoring of pressure vessels. A potential alternative is optical fibers embedded in the vessel's laminate. They have recently been tested as an integrity monitoring tool for fatigue and impact damage, most notably by Munzke *et al.* [20] and Saeter *et al.* [21]. Both studies found that while the technology provided the desired information and gave good indication of the structural integrity, noise and measurement failure from wear on the optical fibers was an issue. In addition, the embedding of the optical fibers into the pressure vessel is an elaborate process. Unlike DIC, optical fibers or strain gauges may only capture the strain in the direction they are mounted, while DIC captures the full field strain in all directions. Post processing signals from optical fibers using the Rayleigh Backscatter method, virtual gauge lengths may be down to 5 mm. The Rayleigh method is the optical fiber post processing method that gives the highest spatial resolution, on par with conventional strain gauges. The virtual gauges may be placed with 1 mm intervals, giving 1.5 mm overlap [21, 22]. The DIC on the other hand have a spatial resolution that is only dependent on the speckle pattern and camera resolution, in theory this may therefor be down to the atomistic level. In practical engineering terms using conventional equipment, the resolution can easily be down to 0.5 mm gauge length, with intervals that can easily be 1/10 of the gauge length, such as used in this study. The only drawback of DIC is that it may not perform measurements at the very high frequency regime which strain gauges may be able to. However, DIC is a rapidly evolving technology and any weaknesses of today may be solved tomorrow. Advanced software is freely available on the net [23–25] and it is seeing a rapid development commercially, such as being embedded in commercial cellphones [26]. It's therefore a technology with a high scientific potential. Identifying its possible appliances, such as for structural health monitoring of pressure vessels and damage development in composites, is the first step on the way to introduce DIC to new fields, where it may give high gains.

This paper investigates mechanical fatigue in a filament wound ring with a hole tested by the split disks method monitored with DIC. The hole was introduced to investigate how fatigue damage evolves around a strain concentrator, simulating damage in a pressure vessel. The study looks into the changes of the surface strain field with increasing number of cycles around several strain concentrators to explain the scatter and evolution of fatigue damage that may be inherent with filament wound materials. This paper also suggests how the DIC post processing methods used may serve as a valuable structural integrity monitoring tool for pressure vessels in use.

2 Experimental setup

2.1 Split disks

The fatigue test was performed on a composite ring cut from a pressure vessel loaded by a split disk in a tension rig. The split disks and the sample had equal dimensions; 50 mm wide and 140 mm in diameter, see schematic in Figure 2. The disks were split by an 11 mm gap, as can be seen in Figure 2. The split disk setup with sample installed can be seen in Figure 3. To minimize the friction between the sample and the disks, industrial grease was used as lubricant. The split disk rig was designed for loads up to 100 kN, roughly twice the testing load.

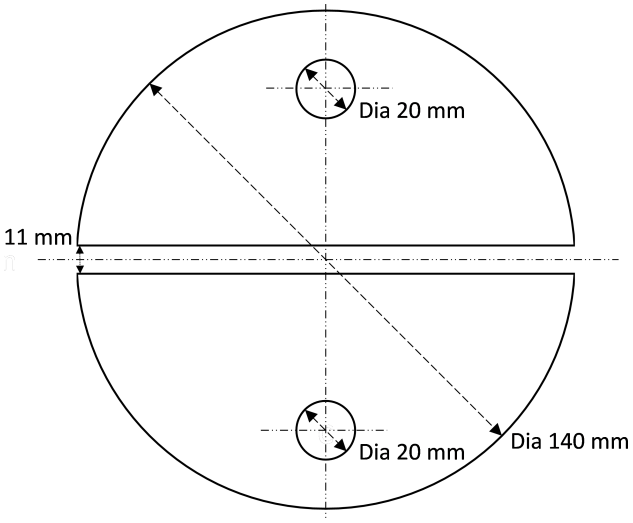

Figure 2: Schematic drawing of the split disks.

Figure 3: Split disk setup with composite ring installed. Cameras on each side and strong lights to provide enough light for the short shutter speed.

2.2 DIC setup

Figure 3 shows the DIC setup, a system from isi-sys. Two cameras were employed, one on each side of the split disk to be sure to capture damage development on both sides. 2D DIC was used as only the area around the hole was of interest, here the total curvature over the camera frame was deemed too low to necessitate 3D DIC. The shutter speed was set as low as possible without compromising brightness. Strong light sources were used to accommodate the short shutter speed. The cameras where synchronized against the test machine's force output, taking pictures at peak load. The image acquisition period (cycles between each picture) was 50 cycles.

The DIC resolution was checked and peak strain was found to converge for the chosen resolution. When using DIC to capture steep strain gradients in high strain areas, some noise will result [27, 28]. A running average over 1000 cycles was used to smooth the strain data in each point.

2.3 Loading scheme

The test sample was fatigue loaded with a sinusoidal load vs. time sequence. The maximum load was 40 kN and the R-ratio was 0.1. Failure occurred at 127815 cycles. The R-ratio of 0.1 is typically used in testing and is a reasonable R-ratio for a pressure vessel in use, with pressures ranging from almost empty to full. The load frequency was set to 1 Hz. This is quite low, but any higher frequency caused excessive frictional heat and subsequent heat affected epoxy, as investigated during preliminary tests on other rings from the same pressure vessel.

3 Materials and fabrication

3.1 Samples

The split disk test sample was cut from a filament wound pressure vessel wound with a layup of $[\pm 89^{\circ}_{2}, \pm 15^{\circ}{}_{1}, \pm 89^{\circ}{}_{2}, \pm 15^{\circ}{}_{1}]$. Using the filament winding production method, it is not possible using conventional approaches to manufacture laminates with exactly straight angles in the hoop direction and particularly the axial direction; which has to be helically wound. 89° (nearly hoop) and 15° (nearly axial) were the highest/lowest angles that were possible to produce without compromising on quality given the filament winding machine and mandrel used. The layup was chosen based on the following requirements.

- Base the layup on a $[\sim 90^\circ, \sim 0^\circ]_n$ layup as this is a commonly used layup in pressure vessels.
- Avoid extensive matrix splitting along the fibers in the loadbearing layers.
- No more than four hoop layers to avoid exceeding the maximum force limit of the test machine.
- Have the inner layer as a non-loadbearing layer to hinder any friction between the splits of the disk and the inner layer affecting the loadbearing layers.
- No more than two helical layers to keep production time within the pot life of the epoxy. (Winding helical layers is time consuming.)
- Keep overall thickness low to hinder too big variation in through thickness strains.

Experience suggests that having only hoop layers in the layup induces extensive matrix splitting along the fibers when testing with the split disk method. Essentially splitting the sample into several smaller samples. This is particularly true for samples with a natural strain concentration inducing shear strains, such as the hole used in this study. Axial layers hinder this behavior as they can transfer some of the shear, particularly if distributed evenly across the layup. With the epoxy, filament winding machine and fiber used in this study the $[\pm 89_2^\circ, \pm 15_1^\circ, \pm 89_2^\circ, \pm 15_1^\circ]$ was judged as being the best compromise given the mentioned constraints.

The geometry of the sample can be seen in Figure 4, θ indicates winding angle. The 20 mm hole was machined with a 20 mm milling tool, 40200-HEMI produced by Seco Tools, which assured minimal fiber and matrix damage around the circumference. To ensure a smooth exit of the tool at the inside of the sample, the holes were machined with a polyethylene liner tightened against the composite ring.

The fiber in the vessel was HiPerTex W2020 produced by 3B [29] with resin Epikote MGS RIMR 135 mixed with curing agent Epikure RIMH 137, both produced by Momentive [30]. The winding mandrel, a 140 mm outer diameter polyethylene pipe with steel domes was cut and extracted after winding. The epoxy does not bond to polyethylene and the coefficient of thermal expansion is higher for the PE than the epoxy, making for easy extraction of the liner when cooled to or below freezing. Curing was done for 15 hours at 80°C.

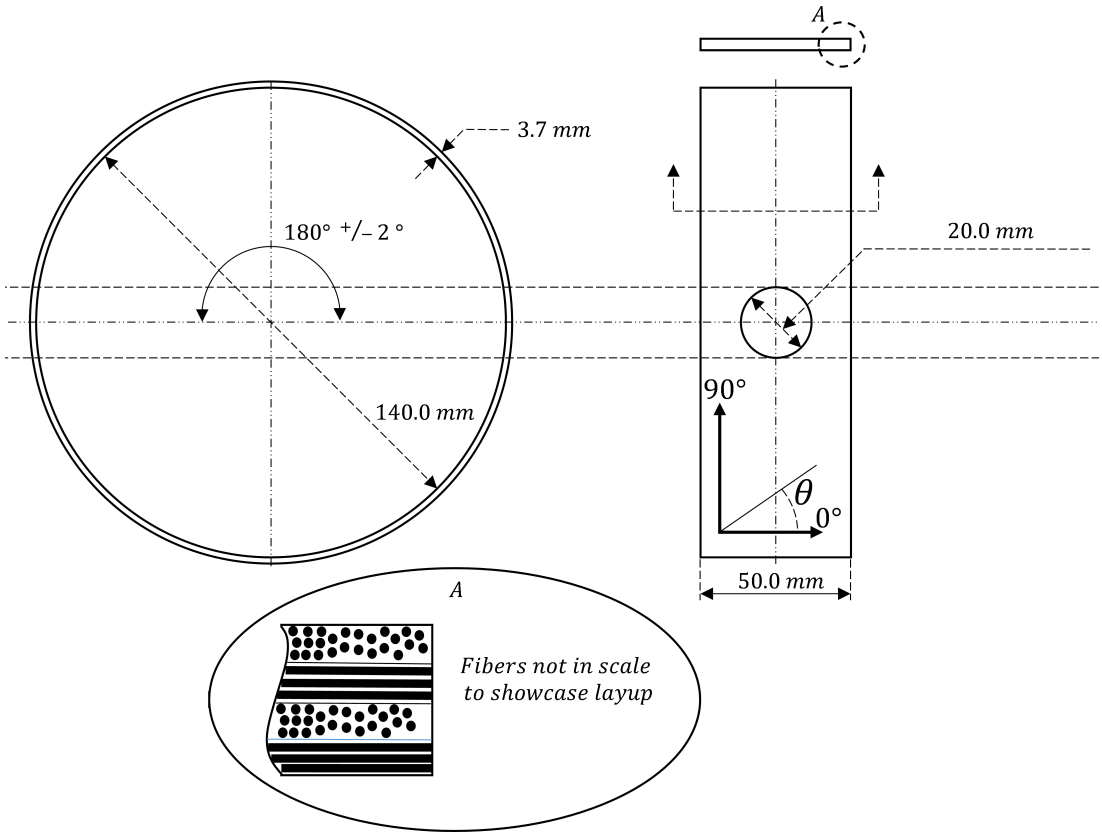

Figure 4: Composite ring sample geometry.

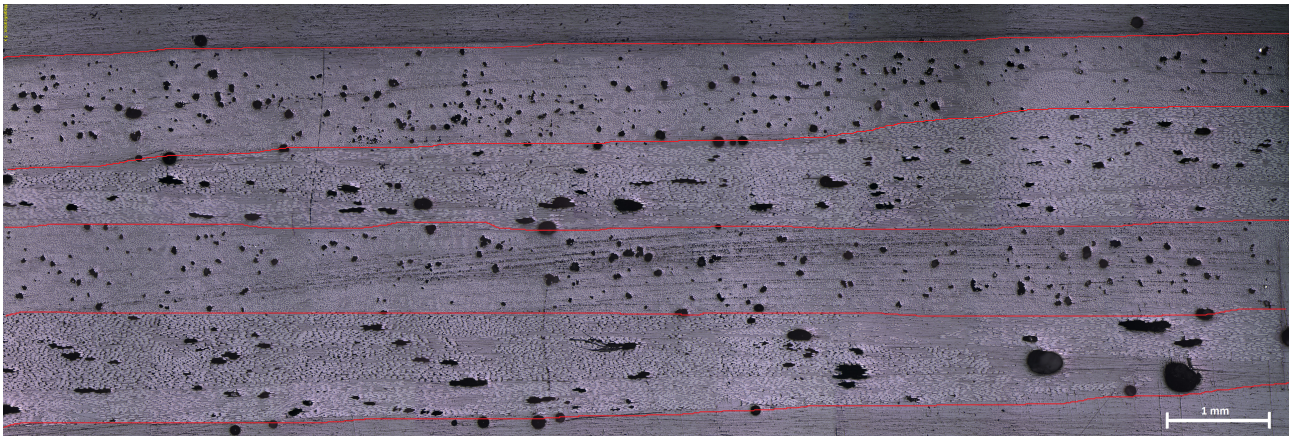

Figure 5: Microscopy of the pressure vessel.

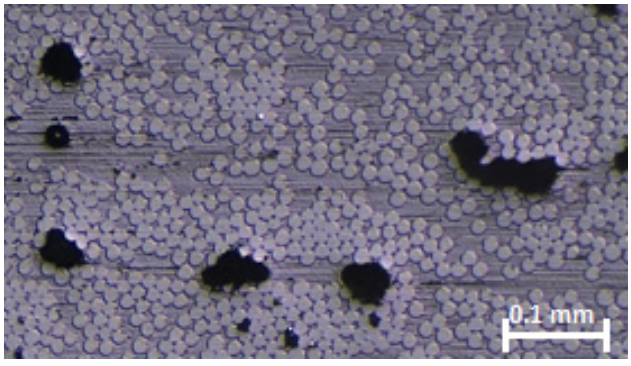

Figure 6: Detailed microscopy showing individual fibers.

3.2 Material characterization

A material characterization was carried out using burn-off testing and microscopy to assess the fiber volume fraction, void content and typical variation in layer thickness. The burn-off test gave a fiber volume fraction of 0.52 using the procedure described in ASTM D3171 – 15 [31]. However, as noted by E. Hugaas [32], when using burn-off testing, any voids will give an artificially high fiber volume fraction. Looking at the microscopy picture in Figure 5 it is evident that the void content is considerable and the actual volume fraction of fibers is consequently lower. Figure 6 shows detailed microscopy down on the individual fiber level. Consequently the actual volume fraction of matrix is also low, while the volume fraction of free space is relatively high. The fiber volume fraction measured here is typical for many structures made by filament winding while it would be high for typical flat panels made by vacuum assisted resin infusion or pre-preg consolidation.

Also evident in the microscopy is a considerable variation in layer thickness. As strain rather than stress is the property of interest for the work in this paper, the volume fraction matters less as the failure strain of the fiber is not affected. However, it will influence the fatigue properties through faster matrix crack growth with more voids [14]. Table 1 shows properties of the used material previously measured by Perillo [10], along with the maximum strain for the fiber from the fiber supplier, 3B [29]. The maximum stress in fiber direction for the data from Perillo was linearly converted to maximum strain by equation (1). Only the maximum fiber strain was available from the fiber supplier as they do not have test data for this particular combination of constituents. As can be seen, there is a big difference between 3B's and Perillo's maximum strain. The deviation is likely due to a more idealized test setup for the supplier's data and more careful handling of the fibers than in the filament winding machine.

Table 1: Material properties.

Material parameter	Value Perillo [10]	Value 3B [29]	Unit
E_1	33.06 (38.6)	-	GPa
X_t	732 (855)	-	MPa
$\hat{\epsilon}_{1t}$	22150 (X_t/E_1)	31000-33000	Microstrain

$$\hat{\epsilon}_{1t} = \frac{X_t}{E_1} \tag{1}$$

4 Results

4.1 DIC

Line slices were used to investigate strain development over the highest strained cross sections. Figure 7 shows schemat-

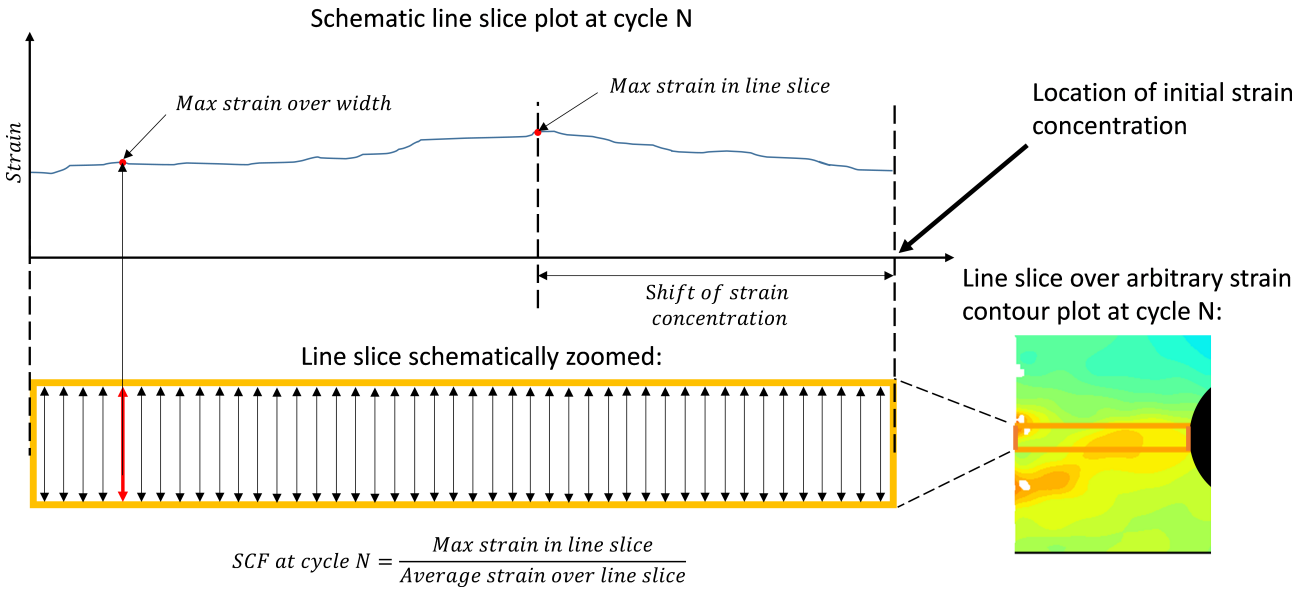

Figure 7: Schematic description of a line slice.

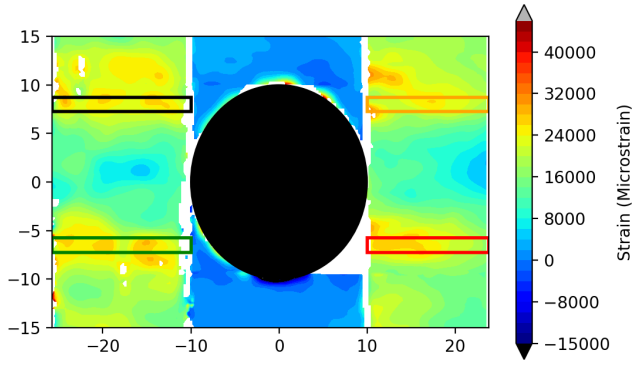

Figure 8: Line slices over hoop strain contour plot at failure. First point of failure in the surface material is indicated by the voids inside the black line slice. Notice also the shear splitting along the tangent to the hole, leaving the center with little load bearing material.

ically how line slices were defined and how the shift of peak strain was defined on the line slices. The peak strain shift was used as a measure of strain field redistribution. Due to the inherent non-uniform strain distribution, line slices had to be defined over a width as well as a length to capture all relevant strain fields that would otherwise be located at the intended line slice provided a perfect material.

The line slices were located at the interesting areas with strain concentrations shown in the contour plot given in Figure 8 for hoop strain within 50 cycles from the failure cycle. Shift of peak strain and Strain Concentration Factor (SCF) plots for the slices can be seen in Figure 9. The peak strain shift zero value is relative to where the peak strain was in the first cycle recorded by the DIC (therefor all strain shifts starts at 0 mm). Catastrophic failure was initiated as fiber failure inside the black line slice indicated by the voids in the left side of the slice. Fiber failures developed over the last 400 cycles before catastrophic failure. Extensive shear splitting along the tangents to the hole can be seen as tangential white voids. The shear splits were initiated already during the first cycle and grew progressively throughout cycling. Note: Bending lowers the strain in the center as depicted in Figure 1.

The strains along the cross section in the line slices with most and least strain redistribution are shown in Figure 10 and Figure 11 for different fatigue cycles. The line slices are the black and orange line slices shown in Figure 8.

4.2 Microscopy

At ultimate failure the ring specimen broke into two parts on only one side near the hole. All strain evaluations presented above were done for the side that failed. The other side had similar partial damage developing near the second hole. This side was used for investigating partial damage by microscopy. Small samples could be cut out and polished for the investigation having internal damage from fatigue that is not affected by the final catastrophic failure happening on the other side of the ring specimen.

Figure 12 shows microscopy from the bottom hoop layer close to the split of the intact side of the ring, a cross section with high strains where it was deemed likely to also find damage. As can be seen there is extensive matrix cracking (red lines) running between voids in the matrix and along

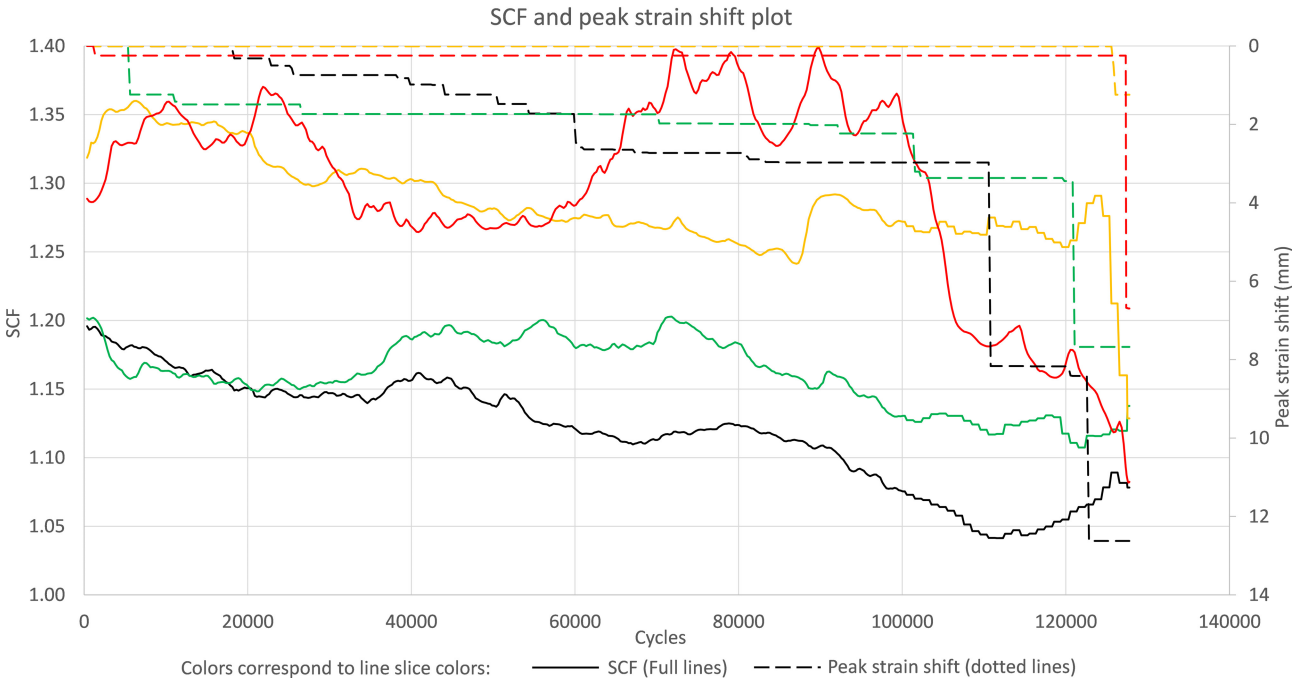

Figure 9: SCF (Maximum strain/average strain) over line slices with the peak strain shift. As can be seen, the SCF is proportional to the redistribution and is steadily falling and lower for the areas with the most redistribution, black and green.

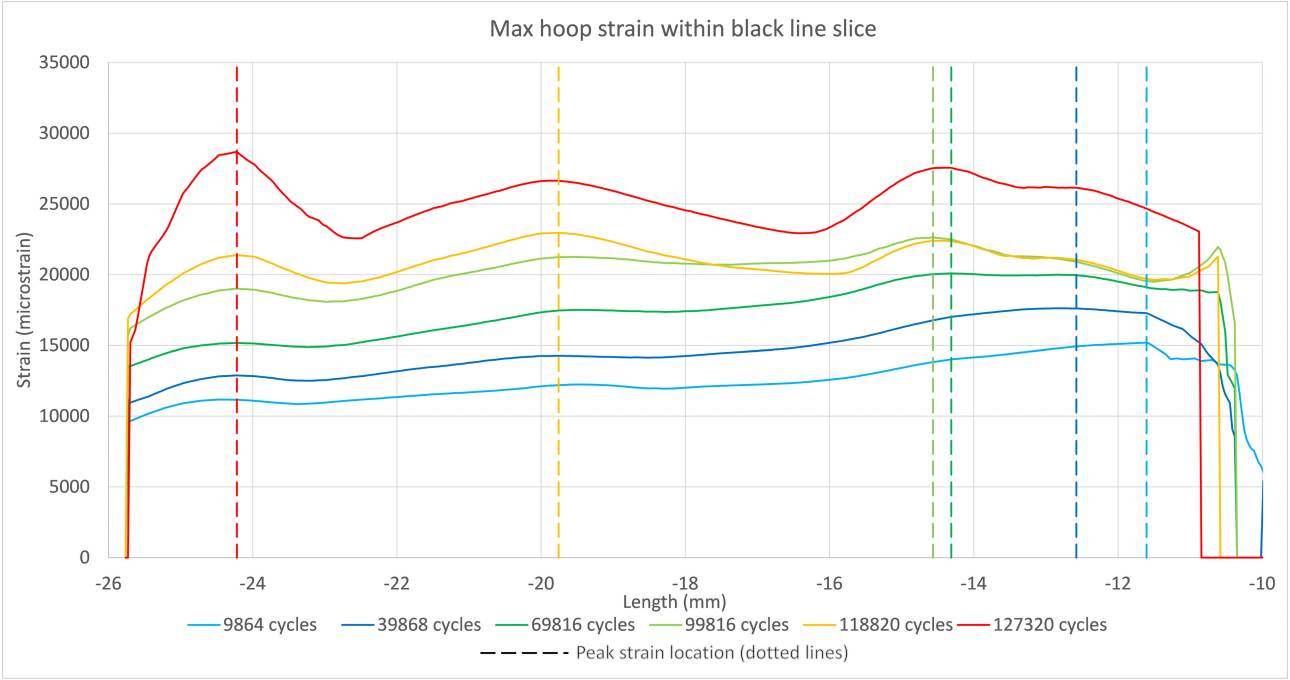

Figure 10: Maximum hoop strain over the black line slice with location of peak strain over the line slice thickness plotted. As can be seen there is extensive redistribution occurring.

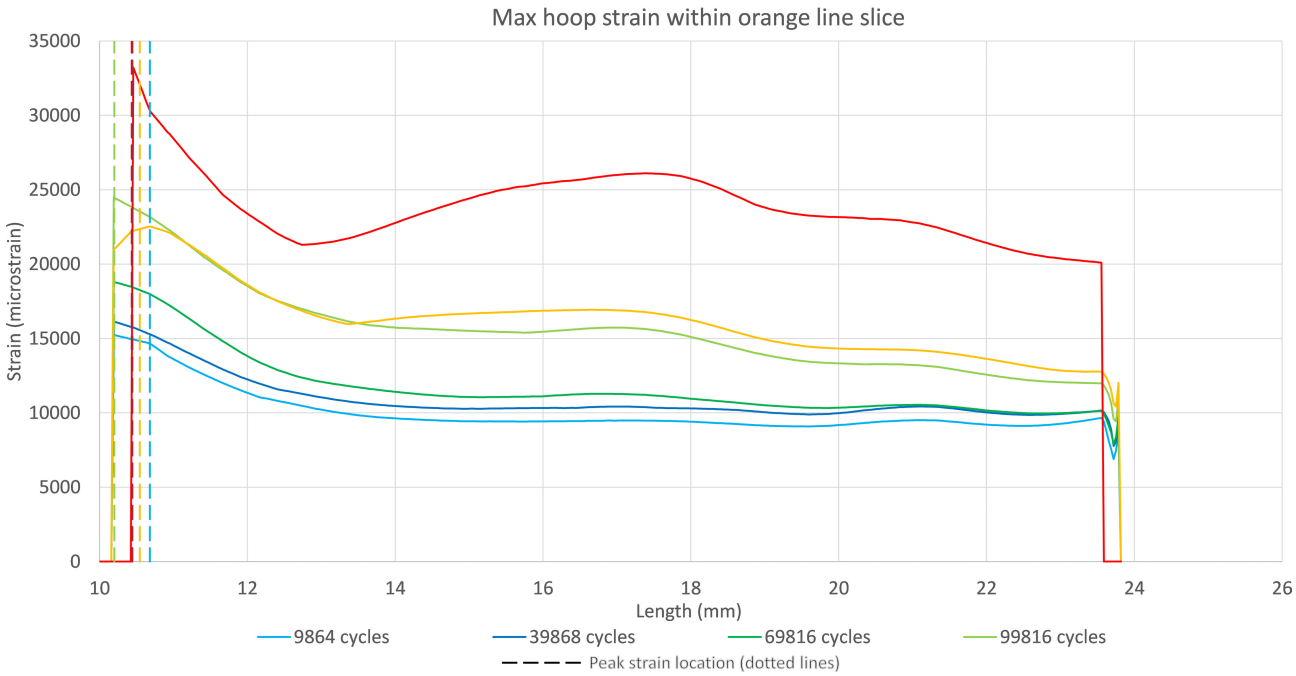

Figure 11: Maximum hoop strain over the orange line slice with location of peak strain plotted, despite high local strains, there is little redistribution due to low strains in the area surrounding peak strain at 10 mm.

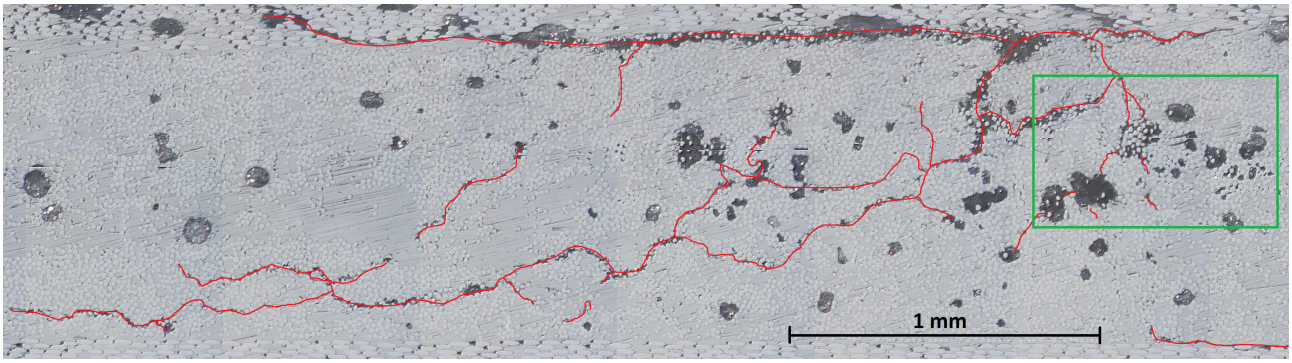

Figure 12: Microscopy of the most strained intact side of the ring with matrix cracks indicated. The green square refers to Figure 13.

the layer interfaces as delamination. This supports the work by Plumtree and Shi [33] and Maragoni *et al.* [12, 14] who found that matrix voids ease matrix cracking in fatigue and that matrix cracks prefer to propagate in between voids.

Figure 13 shows the green area outlined in Figure 12. The areas highlighted in red can be seen to contain debonded fibers and some split of groups of fibers. What may be fractured material can also be seen to be spread as "dust". The matrix splitting and debonding can be seen to have nucleated from the walls of matrix voids and cracks.

Figure 14 shows the fracture, where the DIC results are from. Due to the evidently chaotic nature of the fracture, SEM or microscopy of the fracture was impractical. The microscopy of the damaged material in Figure 12 and Figure 13 was found sufficient to give support to the findings from the strain graphs. The image of the fracture does however highlight where and how catastrophic failure progressed. As can be seen, fiber failure follow the high strain areas in the DIC images outlined with the same colors as in Figure 8. The fiber failures can be seen to "jump" from side to side across the center, likely as an effect of where matrix damage extended across the sample. Inside the black rectangle in Figure 14 it is possible to identify the first fiber failure observed as voids inside the black rectangle in Figure 8, the fiber failure is outlined with red arrows in the figure.

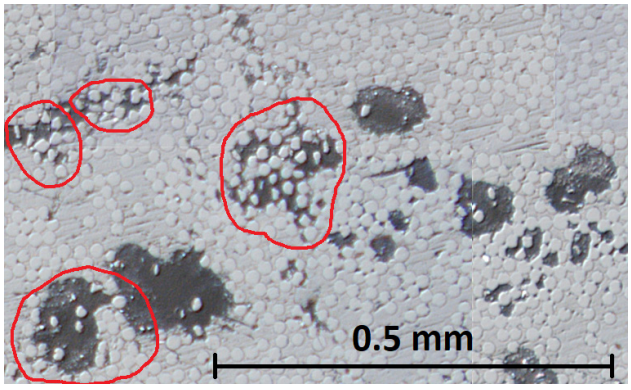

Figure 13: Zoomed area from Figure 12. As can be seen, fiber groups have split from the bulk material and some fibers have completely debonded; here fiber failures can easily interconnect. Red circles highlight the most damaged areas.

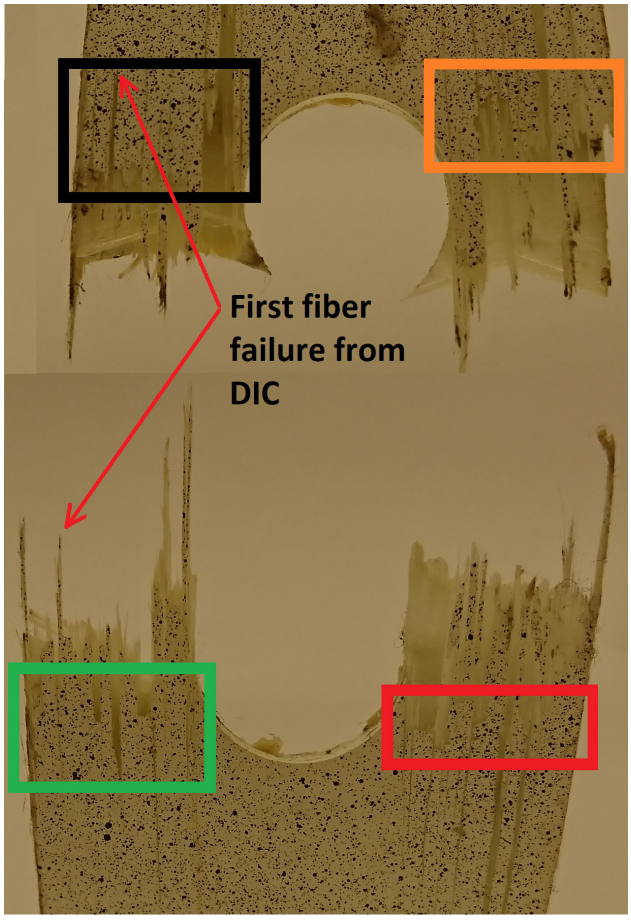

Figure 14: Image of the failed specimen with fiber failure origins outlined in colored squares. The final fracture line runs along both upper and lower side of the specimen and the fiber failures "jump" across the center of the specimen. First fiber failure from the DIC contour plot in Figure 8 is outlined.

4.3 Discussion

There is a varying redistribution of strain near the hole for the different line slices and a marked lowering of the Strain Concentration Factor (SCF), as presented in Figure 9. The largest shift of the position of the peak strain was 12.5 mm happening in the black line slice. The change of SCF was only from 1.2 to 1.05. The highest change in SCF was from about 1.35 to 1.1 for the red and yellow line slices. In both cases the peak strain position remained constant through most of the fatigue life and changed by 6 to 10 mm over the last few hundred cycles. Somewhat surprisingly the first fiber failure happened in the black line slice. This slice has the lowest SCF and lowest peak strain, evident by comparing Figure 10 and Figure 11. The black line slice did however have the highest average strain over the cross section, also evident by comparing Figure 10 and Figure 11.

For fiber failure to progress through the layup and cause loss of structural integrity (catastrophic failure), the matrix has to be sufficiently damaged for fiber failures to coalesce [34, 35]. Considering the fact that fiber failure in this test is sudden, the redistribution of strain is likely an attribute of matrix damage. Supporting this is also the fact that any fiber failure would likely increase the SCF, not lower it, such as for a propagating crack tip. Matrix damage on the other hand reduces the shear stiffness, hindering forces to be transferred between fibers and thus lowering the effect of geometric strain concentrators. The effect is schematically explained in Figure 15. Matrix damage also includes delamination, as indicated in the figure, but which is difficult to measure directly by DIC. The reason why the orange line slice can sustain higher point wise strains than the black is likely due to less matrix damage development, as evident by the smaller strain shift and higher SCF for this area.

For both the orange and the black line slice, peak strain is at or above the ultimate static strain to failure of 22150 microstrain (obtained from standard coupon testing) for a considerable span of cycles, almost 9000 cycles. The orange line slice has strains in the vicinity of the strain to failure reported by the fiber's producer when approaching the last cycles before failure, about 30000-35000 microstrain. This is around 5000 microstrain higher than the black line slice for the same cycle. Again, the orange line slice can likely sustain such high strains due to it having a relatively small amount of matrix damage locally so that any fiber failure may not progress. For both the black and the orange line slices, the high strain relative to the average coupon test strain is an attribute of that the actual strains are measured locally. The strains are not averaged over a larger area or es-

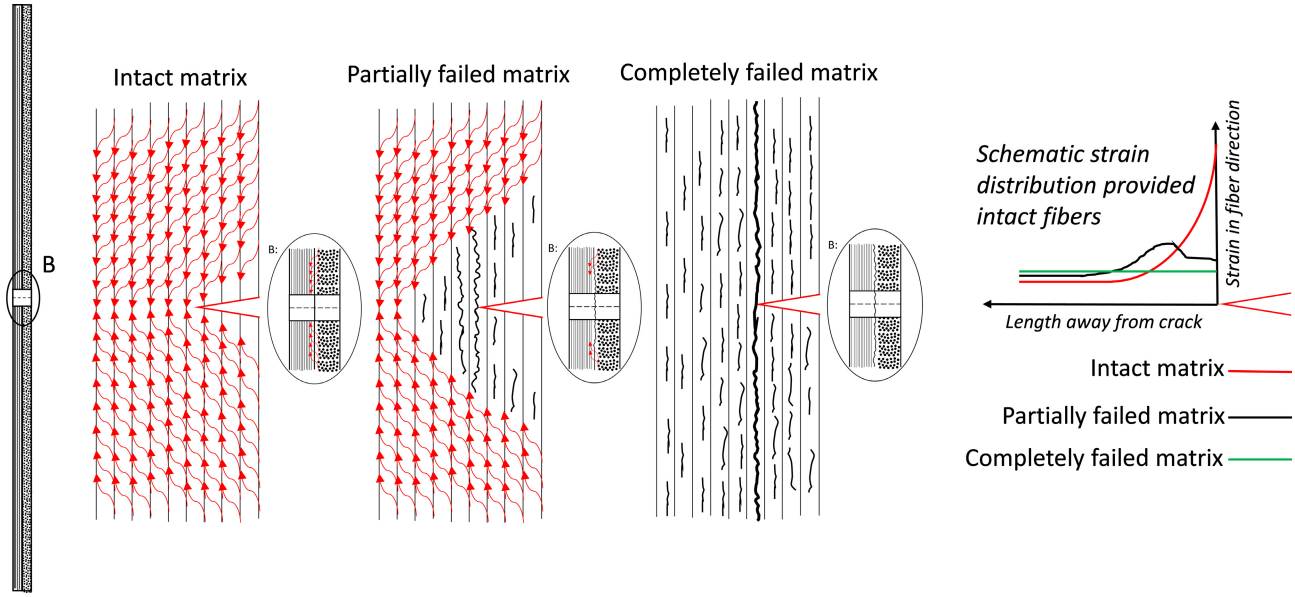

Figure 15: Effect of loss of shear stiffness through matrix damage on the strain distribution around a notch.

timated based on global displacement from a test machine, as in a coupon test.

Looking at the microscopy in Figure 5 the void content is extensive (but typical for many filament wound structures), which is also apparent in the damaged cross section in Figure 12. As evident in Figure 13 fibers and groups of fibers have debonded at matrix cracks and voids, where they are initially free at one side. Compared to the non-fatigued microscopy in Figure 5 and Figure 6 the difference is evident, it contains no cracks and debonding. Debonding is a known failure mechanism in fatigue of composites [33, 36]. The fact that debonding prefers to occur inside voids and along matrix cracks however explains why voids are detrimental to fatigue performance, as concluded by several past studies [11–15]. Not only do voids facilitate faster propagation of matrix cracks, they also serve as nucleus for fiber debonding. The extent of voids in the microscopy further explains why the strain redistribution is extensive and damage apparently matrix driven. Further, the apparent variation in void content, fiber density and layer thickness explains why damage development varies to such a great extent over the specimen. The variation is another attribute of the filament winding production method.

Composites are often used as replacement for steel in design. Fatigue life in design of steel components is usually calculated as life until crack initiation. This is done at hotspots, which are highly stressed points with a geometric strain concentrator [37], such as the hole in this study. Upon crack initiation, damage progression is rapid and the structural integrity is soon lost. Fatigue damage in composites is different, as demonstrated in this study. Fatigue damage initiates in the matrix. Matrix damage does not necessarily evolve at points with a high strain concentration factor, it will prefer to evolve in areas with high overall strain, because this increases the likelihood of a locally weakened matrix (*e.g.* by a void) being exposed to a high strain creating local damage. When the matrix is sufficiently damaged, fiber failure may rapidly progress through the material, comparable to the crack growth phase for steels. While the strain distribution changes little for steel components under fatigue loading before crack initiation, composites may undergo major strain field changes as fatigue matrix damage redistributes strain. Fatigue in composites therefor has an additional phase before the crack initiation phase, the matrix damage phase. This phase has been suggested before [38], but not measured directly on the strain field evolution as here. Depending on the component's shape, laminate buildup and loading condition, this phase may be critical or not. For components designed to withstand shear, matrix cracking is critical. Matrix cracking is not critical in the main cylindrical part of pressure vessels, because the inner liner keeps the vessel tight. The fibers are the load-bearing constituents, especially in a cross ply layup in an even stress/strain field without stress concentration points. In such a layup, matrix damage will lessen the effect of geometric strain concentrators as the strain field redistributes and will be positive in this respect.

An aspect of the presented work that is not taken into account is the size and shape of the introduced defect, and how this may affect the strain fields and damage develop-

ment. While damage progression naturally will vary with the imperfections' geometry it is unlikely that it will deviate on the basic principles outlined here; matrix damage and redistribution. Therefor the aspect of the defect shape and size has not been subject for investigation, finding the failure mechanisms and how they may be monitored is the focus of this work.

Due to the inherent big local variation in void content of filament wound composites and not knowing where the regions with high void content are, matrix damage growth will always be difficult to analytically estimate. Conservative worst-case situations may be modeled, but they may predict quite wrong damage development. Statistical methods may be used to model different distributions of voids, but such models will be complicated. This work has shown that monitoring strains by DIC may be a good alternative to modelling in some cases. As laid out in the introduction it may serve as a good in-service health monitoring tool of composite pressure vessels. Any change in the strain field would be a warning of damage having developed. If the new strain field remains constant with time (increasing number of cycles) it would indicate a somewhat weakened but stable structural integrity. If the strain field changes, the peak strains shift, more severe fiber dominated damage may eventually develop.

Strain monitoring with DIC will always depend on the speckle pattern and resolution of the cameras. The two are the main assumptions for the method's functionality. In this work, the DIC resolution was as fine as possible given the used speckle pattern. Provided a finer speckle pattern, the resolution could naturally have been finer and more detailed strain data acquired. A resolution sensitivity study was however carried out and strain field convergence was found for the chosen resolution. When working in the fine resolution regime of any speckle pattern noise may result [28]. The strength of the used method when working in the fine resolution regime is it's noise reduction over the time dimension, the alternative being smoothing over the space dimension in each frame. When smoothing over the space dimension, strain is compared to the neighboring strain, which will be different from the strain in the data point of interest to start with. When smoothing over time, the strain in the same point should remain reasonably stable over the averaged cycles (here 1000). Any noise reduction will make the strain in the datapoint converge towards the actual value and not the neighboring average strain, as for smoothing over the space dimension. The smoothing over time is only possible due to the high frequency of the data. The necessary resolution when dealing with composites will depend on the material and geometry. For other constituents and geometries the damage development may happen at a smaller scale than for the GFRP material in this work and a higher resolution necessary to find the same mechanisms as here. The question is however at what scale it is necessary to observe damage mechanisms in a material or in a geometry. Damage may occur that is non critical to the strain fields and the structural integrity. In this study, the fact that the strain redistribution clearly develops most extensively for the material sustaining damage first suggests that the resolution is sufficiently fine. Studying strains in the matrix associated directions may also open up for a clearer picture of how the material behave. For this study this was not done out of a scope consideration, but is a good suggestion for further work.

Either standalone or in combination with other health monitoring technologies DIC may serve as a valuable structural integrity tool for pressure vessels. Compared to the optical fiber structural health monitoring method suggested by Munzke *et al.* [20] the presented method has much less noise and is able to give more detailed information on why and how damage develops, at least on the experimental stage. In order for optical fibers or single point strain gauges to catch the same mechanisms, they have to be placed where damage develops and in relatively big numbers. A strain gauge or optical fiber placed where damage was initially thought to develop may therefore not properly catch the strain field development in case the strain field changes with damage. Optical fibers would not be able to give curves with this little noise and this resolution. The fluctuations in the DIC strain would not be possible to catch using 5 mm gauge length, very easily concluded by simply imagining 5 mm strain gauges placed over the x axis in the strain curves in Figures 10–11. Optical fibers with the Rayleigh backscatter method would also not be able to capture strain in anything but a static loadcase. The acquisition time is far longer than the shutter speed of the used cameras for DIC, giving noise if the load is changed during the acquisition. Additionally, for such high strains, the running reference method would have to be used and still then strains in the 30 000 microstrain range would be close to the failure strain of the optical fiber itself [21]. The running reference method would demand stepwise static loading and make fatigue testing extremely time consuming. Strain gauges would be the only practical alternative for monitoring. DIC and strain gauges are hardly comparable as one gauge may give one datapoint out of a thousand or more for the DIC and in only one out of three directions (fiber, matrix and shear). Additionally, the durability issues with the optical fiber reported by Munzke and also Saeter [21] is evidently not a problem with DIC, being much more convenient to implement. On top of all this, the amount of data available when using DIC compared to any other method allows the data processing

competent user to play with the data and find trends that is not possible to discover with other methods, such as the redistribution found in this study. The authors do however recognize that full scale testing may give different results and that strain field development may not be as easy to catch in an industrial vessel as in experiments or in different experimental geometries for that matter. More work is needed testing the methods and technology on actual pressure vessels, also using through thickness methods for comparison.

The DIC system used here is already outdated compared to the cutting edge technological development on the DIC front. It is a technology with big industrial and consumer interest, with algorithms and methods available as open source [23–25] or embedded in commercial hardware such as cell phones, for example for facial recognition [26]. Besides investing more work in quantifying acceptable strain changes, the principles outlined here may serve as a basis for developing a damage detection system relying on an emerging technology with high scientific, industrial and consumer interest. Provided an area of interest in a pressure vessel with known high strains (valve, small damage from use etc.), the post processing concepts outlined in this work may be sufficient information to judge the integrity and potential damage development provided a high resolution image.

5 Conclusion

A split disk fatigue test of a ring with a circular hole cut from a filament wound glass fiber reinforced pressure vessel was carried out. The strain field around the hole was measured by Digital Image Correlation (DIC) at peak load for every 50^{th} cycle. The test lasted 127 000 cycles. It was found that progressive damage in the matrix redistributed strain in the fiber direction throughout the test until catastrophic failure. The redistribution was observed through monitoring Strain Concentration Factors (SCFs) and shift of peak strain location over critical cross sections, both of which lowered and moved with increasing number of fatigue cycles.

While matrix damage redistributed and lowered strain in the direction of the fiber it also eased travel of progressive fiber failure. The area showing most strain redistribution was the area to develop fiber failure first. Other areas with less strain redistribution did not develop fiber failure despite having a higher SCF and strain in the fiber direction in single material points.

Strains could be close to the ultimate strain over considerable cycle spans provided little matrix damage developed locally.

Through microscopy it was found that fatigue damage of the matrix material progressed as debonding of single fibers along borders of matrix cracks and voids. Fatigue of composites occurs in three phases: a stable phase, a matrix damage phase and a sudden fiber failure phase; which marks the end of fatigue life. The strain redistributive behavior of the matrix damage phase may be advantageous in fatigue sensitive applications creating a stable and evenly distributed strain field. Matrix damage may lower strain around any damaged area and make it converge to the far field strain over time, removing the initial strain concentration. Better control of the structural integrity and higher confidence in lifetime evaluations may result from monitoring damaged areas and weak spots in commercial pressure vessels with DIC combined with the post processing methods presented in this study. Considering the rapid growth of image recognition technology, research on such technology for structural integrity monitoring may yield high scientific and commercial gains.

Acknowledgement: This work was performed within MoZEES, a Norwegian Centre for Environment-friendly Energy Research (FME), co-sponsored by the Research Council of Norway (project number 257653) and 40 partners from research, industry and public sector.

References

[1] IEA Hydrogen, Global trends and outlook for hydrogen, IEA Hydrogen, 2017.
[2] J. Degrieck and W. V. Paepegem, "Fatigue Damage Modelling of Fibre-reinforced Composite Materials: Review," *Applied Mechanics Reviews*, vol. 54, no. 4, pp. 279-300, 2001.
[3] ISO, ISO 11515:2013 (Confirmed in 2019), ISO – International Organization for Standardization, 2019.
[4] ISO, ISO 11119-3:2013 (Confirmed in 2018), ISO – International Organization for Standardization, 2018.
[5] J.-P. Antoniotti, "Impact of high capacity CGH2-trailers," *Deliverable 6.4 in EU research project DeliverHy*, 2013.
[6] J. P. Berro Ramirez, D. Halm, J.-C. Grandidier, S. Villalonga and F. Nony, "700 bar type IV high pressure hydrogen storage vessel burst – Simulation and experimental validation," *International Journal of Hydrogen Energy*, vol. 40, no. 38, 2015.
[7] I. A. Jones, V. Middleton and M. J. Owen, "Roller-assisted variant of the split disc test for filament-wound composites," *Composites Part A: Applied Science and Manufacturing*, vol. 27, no. 4, pp. 287-294, 1996.
[8] C. Kaynak, E. S. Erdiller, L. Parnas and F. Senel, "Use of split-disk tests for the process parameters of filament wound epoxy

composite tubes," *Polymer Testing*, vol. 24, no. 5, p. 648–655, 2005.

[9] J. F. Chen, S. Q. Li, L. A. Bisby and J. Ai, "FRP rupture strains in the split-disk test," *Composites Part B: Engineering*, vol. 42, no. 4, pp. 962-972, 2011.

[10] G. Perillo, Numerical and Experimental Investigation of Impact Behaviour of GFRP Composiites (PhD thesis)., Trondheim: NTNU – Norwegian University of Science and Technology, 2014.

[11] S. M. Sisodia, E. K. Gamstedt, F. Edgren and J. Varna, "Effects of voids on quasi-static and tension fatigue behaviour of carbon-fibre composite laminates," *Journal of Composite Materials*, vol. 49, no. 17, pp. 2137-2148, 2015.

[12] L. Maragoni, P. A. Carraro, M. Peron and M. Quaresimin, "Fatigue behaviour of glass/epoxy laminates in the presence of voids," *International Journal of Fatigue*, vol. 95, pp. 18-28, 2017.

[13] J. Lambert, A. R. Chambers, I. Sinclair and S. M. Spearing, "3D damage characterisation and the role of voids in the fatigue of wind turbine blade materials," *Composite Science and Technology*, vol. 72, no. 2, pp. 337-343, 2012.

[14] L. Maragoni, P. A. Carraro and M. Quaresimin, "Effect of voids on the crack formation in a [45/−45/0]s laminate under cyclic axial tension," *Composites Part A: Applied Science and Manufacturing*, Vols. 91, Part 2, pp. 493-500, 2016.

[15] M. Mehdikhani, L. Gorbatikh, I. Veerpost and S. V. Lomov, "Voids in fiber-reinforced polymer composites: A review on their formation, characteristics, and effects on mechanical performance," *Journal of Composite Materials*, vol. 53, no. 12, pp. 1579-1669, 2018.

[16] W. R. Broughton, M. R. L. Gower, M. J. Lodeiro, G. D. Pilkington and M. R. Shaw, "An experimental assessment of open-hole tension–tension fatigue behaviour of GFRP laminate," *Composites Part A: Applied Science and Manufacturing*, vol. 42, no. 10, pp. 1310-1320, 2011.

[17] A. Muc, "Design of composite structures under cyclic loads," *Computers & Structures*, vol. 76, no. 1-3, pp. 211-218, 2000.

[18] S. Giancane, F. W. Panella, R. Nobile and R. Dattoma, "Fatigue damage evolution of fiber reinforced composites with digital image correlation analysis," *Procedia Engineering 2*, vol. 2, no. 1, pp. 1307-1315, 2010.

[19] T. He, L. Liu and A. Makeev, "Uncertainty analysis in composite material properties characterization using digital image correlation and finite element model updating," *Composite Structures*, vol. 184, pp. 337-351, 2018.

[20] D. Munzke, E. Duffner, R. Eisermann, M. Schukar, A. Schoppa, M. Szczepaniak, J. Strohhäcker and G. Mair, "Monitoring of type IV composite pressure vessels with multilayer fully integrated optical fiber based distributed strain sensing," *Materials Today: Proceedings*, 2020.

[21] E. Saeter, K. Lasn, F. Nony and A. T. Echtermeyer, "Embedded optical fibres for monitoring pressurization and impact of filament wound cylinders," *Composite Structures*, vol. 210, pp. 608-617, 2019.

[22] E. Hugaas, A. T. Echtermeyer and N. P. Vedvik, "Buckling due to external pressure of a composite tube measured by Rayleigh optical backscatter reflectometry and analyzed by finite elements," *Structural Control and Health Monitoring: The Bulletin of ACS*, vol. 25, no. 8, 2018.

[23] S. Nordmark Olufsen, M. E. Andersen and E. Fagerholt, "(mu)DIC: An open-source toolkit for digital image correlation," *SoftwareX*, vol. 11, p. 100391, 2020.

[24] J. Blaber, B. Adair and A. Antoniou, "Ncorr: Open-Source 2D Digital Image Correlation Matlab Software," *Society for Experimental Mechanics*, vol. 55, pp. 1105-1122, 2015.

[25] D. Solav, K. M. Moerman, A. M. Jaeger, K. Genovese and H. M. Herr, "MultiDIC: An Open-Source Toolbox for Multi-View 3D Digital Image Correlation," *IEEE Access*, vol. 6, pp. 30520-30535, 2018.

[26] D. Guillaume, X. Chao and K. Sriadibhatla, "Face Recognition in Mobile Phones," Department of Electrical Engineering, Stanford University, 2010.

[27] "Digital Image Correlation," Will LePage, [Online]. Available: https://digitalimagecorrelation.org/. [Accessed 12 May 2019].

[28] N. McCormick and J. Lord, "Digital Image Correlation," *Materials today*, vol. 13, no. 12, pp. 52-54, 2010.

[29] 3B, "HiPertex W2020 datasheet," 3B, 2015.

[30] Momentive, Technical Datasheet Epikote Resin MGS RIMR 135 and Epikure Curing Agent MGS RIMH 134 – RIMH 137, Momentive, 2006.

[31] ASTM, ASTM Standard D3171 – 15 Standard Test Methods for Constituent Content of Composite Materials, ASTM, 2015.

[32] E. Hugaas, Optimize resistance to buckling under external hydrostatic pressure of thin walled composite tubes. (Master thesis), Trondheim: NTNU, 2014.

[33] A. Plumtrée and L. Shi, "Fatigue damage evolution in off-axis unidirectional CFRP," *International Journal of Fatigue*, vol. 24, no. 2-4, pp. 155-159, 2002.

[34] H. Y. Chou, A. R. Bunsell and A. Thionnet, "Visual indicator for the detection of end-of-life criterion for composite high pressure vessels for hydrogen storage," *International Journal of Hydrogen Energy*, vol. 37, no. 21, pp. 16247-16255, 2012.

[35] R. Talreja and W. Watt, "Fatigue of composite materials: damage mechanisms and fatigue-life diagrams," *Proceedings of the Royal Society A*, vol. 378, no. 1775, pp. 461-475, 1981.

[36] A. T. Seyhan, "A Statistical Study of Fatigue Life Prediction of Fibre Reinforced Polymer Composites," *Polymers & Polymer Composites*, vol. 19, no. 9, pp. 717-723, 2011.

[37] DNV GL, DNVGL-RP-C203 Fatigue design of offshore steel structures, Høvik: DNV GL, 2019.

[38] C. Colombo, F. Libonati and L. Vergani, "Fatigue damage in GFRP," *International Journal of Structural Integrity*, vol. 3, no. 4, pp. 424-440, 2012.